Journal of Marine Science and Technology

Volume 22 | Issue 5 Article 9

FLAME BEHAVIOR OF BIFURCATED JETS IN A V-SHAPED BLUFF-BODY BURNER

Hsiu Feng Yang
Department of Mechanical Engineering, Taipei Chenshih University of Science and Technology, Taipei, Taiwan, R.O.C

Ching Min Hsu
Graduate Institute of Applied Science and Technology, National Taiwan University of Science and Technology, Taipei, Taiwan, R.O.C.

Rong Fung Huang
Department of Mechanical Engineering, National Taiwan University of Science and Technology, Taipei, Taiwan, R.O.C., rfhuang@mail.ntust.edu.tw

Recommended Citation

Yang, Hsiu Feng; Hsu, Ching Min; and Huang, Rong Fung (2014) "FLAME BEHAVIOR OF BIFURCATED JETS IN A V-SHAPED BLUFF-BODY BURNER," *Journal of Marine Science and Technology*: Vol. 22: Iss. 5, Article 9.
DOI: 10.6119/JMST-013-1025-1
Available at: https://jmstt.ntou.edu.tw/journal/vol22/iss5/9

Journal of Marine Science and Technology, Vol. 22, No. 5, pp. 606-611 (2014)
DOI: 10.6119/JMST-013-1025-1

FLAME BEHAVIOR OF BIFURCATED JETS IN A V-SHAPED BLUFF-BODY BURNER

Hsiu Feng Yang[1], Ching Min Hsu[2], and Rong Fung Huang[3]

Key words: V-shaped bluff-body burner, bifurcated jets, flame behavior.

ABSTRACT

A plane fuel jet bifurcated into two streams of jets by a V-shaped bluff-body burner with co-flowing air streams was studied. The flame behavior, length, and temperature distributions of the bifurcated jets were experimentally examined. Flame behavior was characterized by flame visualization and instantaneous photograph. The flame length characteristics was obtained by using the long-exposure flame images. The temperatures distributions were measured by using a fine-wire thermocouple. Three characteristic flame modes were revealed—*attached flame*, *transitional flame*, and *lifted flame*. The flame length and width of the bifurcated jets increase with the increase of the Re_c in fixed Re_a. The length of the bifurcated flame was significantly shorter than that of the plane jet flame. The reduction was induced by the enhancement in the mixing and entrainment effects of the bifurcated flame. The maximum temperature of the bifurcated-jets flame decreases with the increase of the Re_c. The bifurcated jets enhanced the mixing of the fuel and the air and improved the combustion efficiency. The flame behavior and combustion characteristics of the bifurcated jets changed drastically due to the effects of entrainment and recirculation.

I. INTRODUCTION

In many industrial applications, a plane jet is used for mixing, heat transfer, combustion, etc. The axial momentum of a natural plane jet is drastically stronger than the lateral momentum and therefore the transport properties in the lateral direction are negligibly smaller than those in the axial direction. The jet fluids must convect to far downstream area so that the mixing induced by entrainment effect and breakup of large-scale coherent flow structure becomes effective. This deficit causes difficulties in fast mixing in the near field. The plane jet, thus, is usually modified to enhance its transport properties in terms of momentum, heat, and mass transfers. The literature (e.g., [1, 4, 12]) reports that flow-control techniques for a jet, such as the acoustic excitation, jet exit tripping, and nozzle exit shaping, can enhance a jet's turbulence fluctuation, entrainment, and mixing.

The V-shaped bluff-body is one of the modifications for a plane jet that is widely used in many of the combustion apparatuses due to its effective flame-holding ability and low pressure-loss characteristics [5]. For example, it is used in gas turbine combustors, ramjet combustors, thrust augmenters, afterburner, boilers, furnaces, etc. The fundamental ideas of the application of V-shaped bluff-body wakes in combustors are (1) to benefit from the reverse flow in the near field that causes the expedition of the mixing process and to stabilize the flame, (2) to provide high temperature from the burnt products in recirculation zone that can ignite the fresh mixture continuously, and (3) to enhance the mixing of the fuel and air by entrainment that improves the combustion efficiency [2, 6, 7, 11, 13].

A plane jet can be bifurcated into two streams by passing the jet fluids through a V-shaped bluff body which contains two slits on the downstream face of the V-shaped bluff body to serve as the exits of the bifurcated jets. The bifurcated jets issued from the slits of the V-shaped bluff body would merge into one free plane jet in the downstream area and caused recirculation bubble and large turbulence, and in turn induced significant lateral dispersion of the axial momentum. The flow structure have been studied previously by many investigators on the subject relevant to two parallel plane jets [3, 8-10]. The induced recirculation is expected to enhance mixing between the jet fluids and the environmental air, and therefore, if applied to the burners, could enhance combustion and flame stabilization characteristics.

In this study, we installed a V-shaped bluff-body burner on the exit of a plane jet. The fuel flowed through a narrow rectangular channel, directed into the inlet of the V-shaped bluff-body burner, bifurcated into two fuel jets, and issued out of the slits on the downstream face of the bluff body.

Paper submitted 08/19/12; accepted 10/25/13. Author for correspondence: Rong Fung Huang (e-mail: rfhuang@mail.ntust.edu.tw).
[1] *Department of Mechanical Engineering, Taipei Chenshih University of Science and Technology, Taipei, Taiwan, R.O.C.*
[2] *Graduate Institute of Applied Science and Technology, National Taiwan University of Science and Technology, Taipei, Taiwan, R.O.C.*
[3] *Department of Mechanical Engineering, National Taiwan University of Science and Technology, Taipei, Taiwan, R.O.C.*

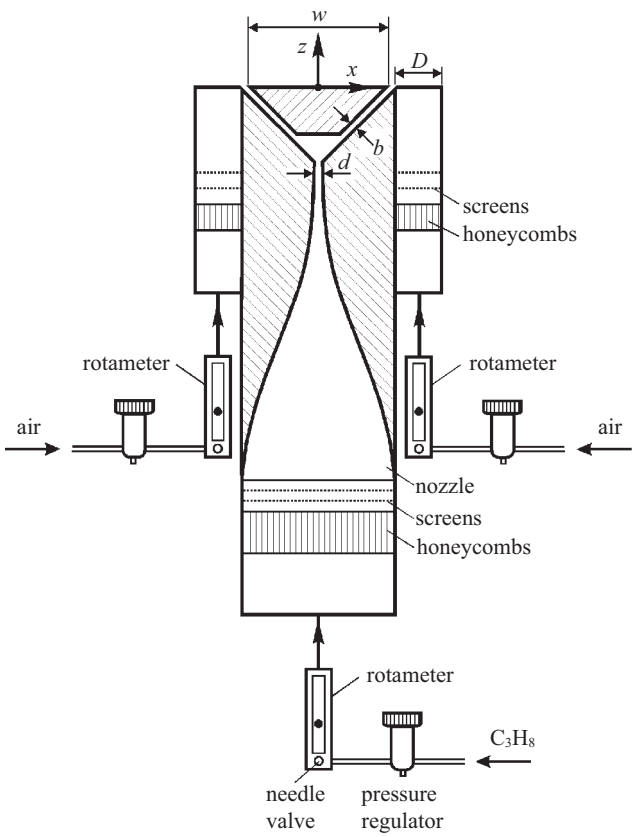

Fig. 1. Experimental setup.

Co-flowing air streams were supplied with two planar air jets arranged next to the V-shaped bluff body. The aerodynamics of the flow field induced by the interaction of the bifurcated fuel jets, co-flowing air jets, and V-shaped bluff body would be characterized by complex vortex structures in the wake region. This complex vortex structures would enhance the mixing capability and turbulence intensity of the flow and may improve the combustion efficiency. The present paper first described the flame behavior of the bifurcated fuel jets and categorized the characteristic flame modes. Then it described the thermal structure of the bifurcated-jet flames. Finally, it discussed the differences between the characteristic flame modes.

II. EXPERIMENTAL METHODS

1. Burner Configurations

Fig. 1 shows the V-shaped bluff-body burner developed to bifurcate a plane jet into two planar streams jets. The fuel gas was supplied through a rectangular channel (installed with a honeycomb and screens for filtering the draft), passed through a nozzle with a fifth-order polynomial profile, went through a narrow channel with a width d of 2 mm, and was injected into a target blockage which had a flat surface facing to the inlet of the jet. The target blockage was placed between two side plates which were configured in a Y shape, and therefore formed two passages for venting of the bifurcated jets. The target blockage and the two side plates were made of stainless steel. The target blockage had a downstream width w = 35 mm. The width of the side passages was b = 1 mm. Since the angle between two side plates was 45°, the width of the slits on the downstream face of the target blockage was 1.4 mm. The origin of the coordinate system (x, y, z) was located at the centre of the downstream surface of the target blockage. The span length s of the burner in the direction y was 165 mm. Two rectangular channels with a width D = 11 mm stood along the sides of the burner to provide co-flowing air flows. A ring blower was used to provide the co-flowing air flows. In order to minimize the flow perturbation caused by the rotating blower blades, acoustic filters were installed downstream of the exit of the ring blower. The fuel gas came from a propane pressure tank. It was commercial grade propane with composition of about 95.0% C_3H_8, 3.5% C_2H_6, and 1.5% C4H10. Before the fuel gas and co-flowing air were fed into the test rig, they were quantified via rotameters that were calibrated by a micro-pressure calibration system to an accuracy of 1% of full scale. The fuel gas and co-flowing air were passed through the honeycombs and screens before going into the test rig in order to reduce the drafts.

2. Flame Visualization

The flame images were acquired by a Sony CCD progressive-scan camera (DCR-TRV 900NTSC). This image acquisition tool had a frame rate fixed at 30 frames per second, but the camera shutter speed was varied depending on the type of flame whose image was being captured. In order to measure the flame length, a long-exposure photographic technique was adopted by using a Nikon still camera (Nikon COOLPIX 990). The flame length was measured by averaging 40 flame photos with an exposure time of 1 second. In other words, the flame-length data presented the average of 40 seconds exposure time. Experiments using various exposure times and number of pictures for average were conducted. The results suggested that 15 seconds of exposure time was enough to yield a stable average value for all flame behaviors.

3. Temperature Measurement

The temperature measurements were carried out with a data logger coupled with a personal computer (KEITHLEY Instruments, model 2750). The probe used was a homemade type-R thermocouple. The wire diameter was 125 μm. The diameter of the spark-welded bead was approximately 175 μm. The measuring bead protruded 2 cm away from the tip of its 2 mm diameter ceramic stem. This ceramic stem was securely fastened to an L-shaped stainless steel tube where the plug was attached. The probe assembly was positioned in the test section through the aid of a traversing mechanism that had a minimum step resolution of 10 μm. In total, 5000 data at a sampling rate of 50 Hz were collected for each measurement, depending on the location in the reaction zone. The flame was

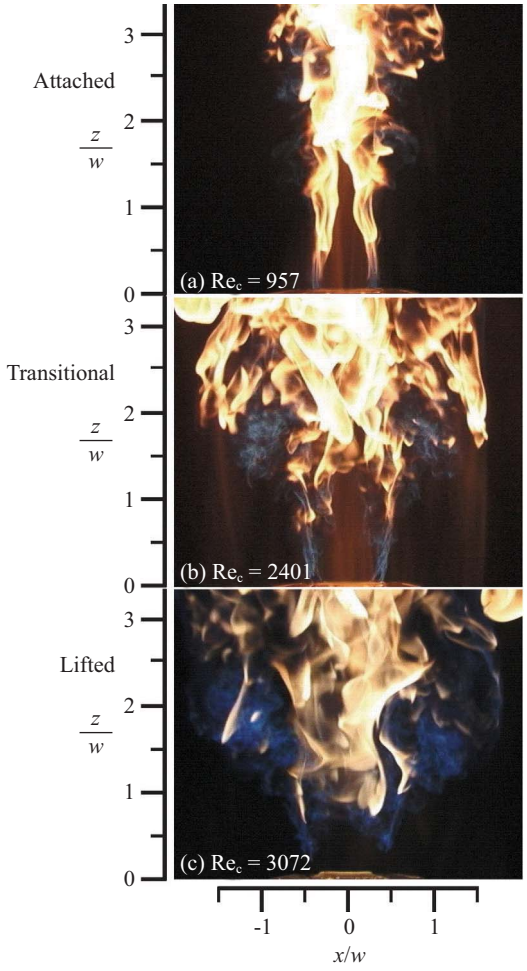

Fig. 2. Flame appearances near exit of burner. Re_a = 1334. (a) attached flame, (b) transitional flame, (c) lifted flame. Exposure time 1 ms.

guarded by three layers of mesh screen to resolve the effects of room drafts and other disturbances inside the laboratory.

III. RESULTS AND DISCUSSION

1. Appearances of Flames

Fig. 2 shows three typical flames near the exit of the burner observed in the *y* direction. The Reynolds number of the co-flowing air Re_a is 1334, where $Re_a = u_a D/v_a$, in which u_a is the volumetric mean velocity of the co-flowing air at the exit of the air channel, v_a is the kinematic viscosity of air, and D is the width of the air channel. In Fig. 2(a), at the low Reynolds number Re_c = 957 (where $Re_c = u_c d/v_c$, in which u_c is the volumetric mean velocity of the central planar fuel jet, v_c is the kinematic viscosity of fuel, and d is the width of central fuel channel) each bifurcated fuel jet issuing from the side slit of the burner forms a diffusion flame. The two diffusion flames attract each other and deflect toward the center plane. The two reacting jets may have a similar physical mechanism to two parallel plane jets [3, 8-10]—the jets would merge at a distance downstream from the jet exits and form a recirculation bubble in the wake. The merged jets would develop into a free jet in the downstream area. Such a flow structure therefore causes the separated diffusion flames starting to merge at $z/w \approx 1.5$ and become a single flame in the downstream area after $z/w \approx 2$. No flames are observed in the dark, triangular area (i.e., the converging region) before mergence of the diffusion flames. The image in the area $z/w > 2$ shows a single turbulent flame. Downstream of the mergence of the two slit-jet flames, the flame width expands abruptly. The flame induced by the combined jet shows stronger turbulence and wider appearance.

At the mediate Reynolds number Re_c = 2401, as shown in Fig. 2(b). The blue diffusion flames near the burner go almost upright. No flames are observed in the space between the two blue flames, which exhibit the characteristics of diffusion flame. At this Reynolds number, the base of the blue diffusion flames actually exhibits an unsteady lifting and reattaching motion at the exit of the burner. At $z/w \approx 1.3$, the two blue flames start to merge toward the center axis and finally finishes the mergence at $z/w \approx 2$. At $z/w \approx 1.3$, where the flames start to merge, the flames expand abruptly and become much wider than the flame at $z/w < 1.3$. The abruptly widened flame is accompanied with large turbulent fluctuations. In addition to the diffusion flames appearing near the burner exit, more blue flames are observed around the base of the suddenly widened flames in the region $1.3 < z/w < 2$. The sudden expansion of the flames at $z/w \approx 1.3$ may be induced by the phenomenon that the merged jets always expands laterally downstream of the stagnation point [3, 8-10].

At the large Reynolds number Re_c = 3072, as shown in Fig. 2(c), the blue diffusion flames lift off the burner and stand at a short distance about $0.2w$ away from the burner. The mergence point of the flames is lowered down to $z/w \approx 0.8$, and the merged flame expands laterally suddenly around that level. The flames become drastically wider with larger blue zones and stronger turbulence. In Fig. 2, the level of the mergence point decreases with the increase of Re_c. The different appearances of the flames shown in Figs. 2(a), (b) and (c) are termed attached, transitional and lifted flames, respectively.

Fig. 3 exhibits the instantaneous full flame appearance of the bifurcated jets corresponding to Fig. 2. The images are taken at an exposure time of 1 ms. In Figs. 3(a)-(c), the images present more turbulent and more blue flames in the region $z/w < 10$ where primary reaction takes place. Defining a length ratio LR as the ratios of the length of the primary reaction zone to the length of the whole flame. The values of LR are about 33%, 20%, and 18%, respectively, for the attached, transitional, and lifted flames shown in Fig. 3. The attached flame has the highest length ratio among the three characteristic flame modes. This may indicate that the attached flame requires a longer axial distance for completing reaction. For transitional and lifted flames, the reaction could be completed within a shorted distance, which means the diffusion and mixing in the near field of the transitional and lifted flames are

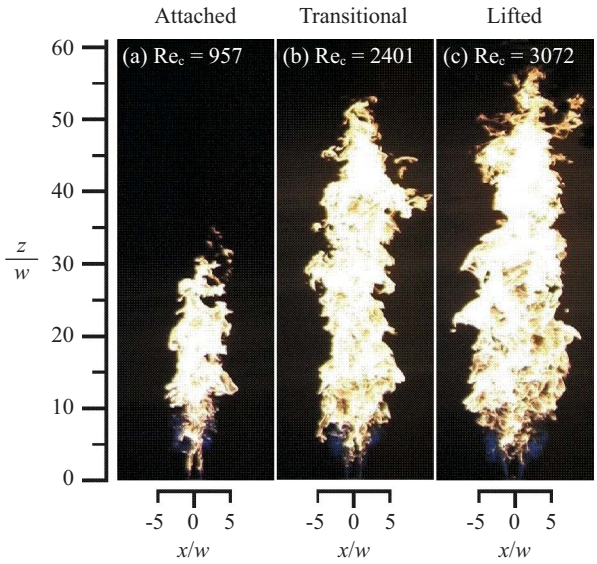

Fig. 3. Instantaneous full-length flame appearances. Re$_a$ = 1334. Exposure time 1 ms.

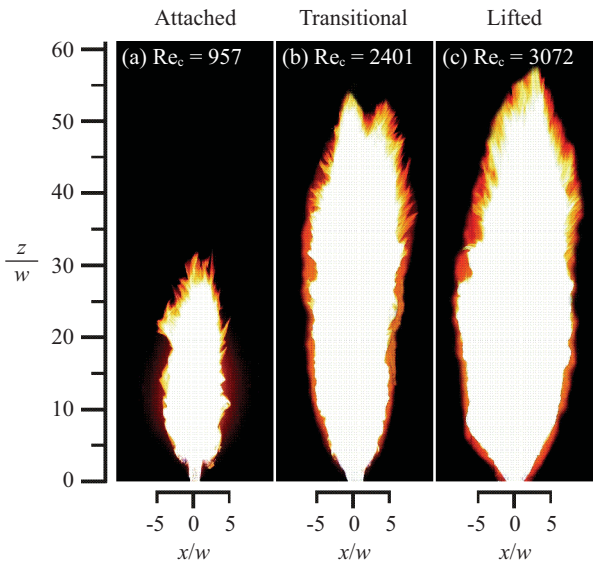

Fig. 4. Long exposure full-length flame appearances. Re$_a$ = 1334. Exposure time 1 s.

more intensive than those of the attached flame. The enhancement of the reaction (due to the enhancement of mixing and diffusion) in the transitional and lifted flames can be cross-references from the increase of the flame width within the reaction zone. Fig. 4 shows the long-exposure pictures of full flame appearances corresponding to Fig. 3. It is apparent that the flame length and width increase with the increase of Re$_c$ at a fixed Re$_a$ = 1334.

2. Regimes of Characteristic Flame Modes

The characteristic flame regimes are identified in the domain of Re$_c$ and Re$_a$, as shown in Fig. 5. The narrow bands

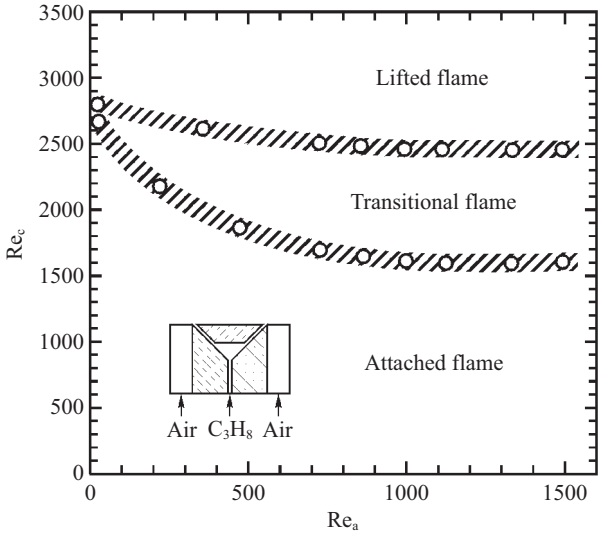

Fig. 5. Regimes of characteristic flame modes.

composed of short back-slashed lines denote the borders separating two different characteristic flame modes. We obtained the borders by examining the flame images of pictures. The width of the narrow bands delineates the uncertainty of the mode identification. For Re$_a$ > 800, the borders do not change significantly with variation of Re$_a$. The borders separating the *attached flame* and the *transitional flame* regimes as well as the *transitional flame* and *lifted flame* regimes are about Re$_c$ ≈ 1600 and 2400, respectively, for Re$_a$ > 800. For Re$_a$ < 800, the border between the *attached flame* and the *transitional flame* regimes varies with Rea that the lower the Re$_a$, the larger the critical Re$_c$. This implies that the flame at larger co-flowing velocity Rea is easier to lift off the burner than at smaller Re$_a$.

3. Flame Lengths

The dimensionless flame length H_f /w of the bifurcated jets at various Re$_a$ are shown in Fig. 6. The bands composed of short slashed lines show the borders between different characteristic flame modes. In the regime of the attached flame, the flame length increases rapidly with the increase of Re$_c$. The length of the attached flame may increase from about 29w at Re$_c$ ≈ 1000 to about 43w at Re$_c$ ≈ 1500. Increasing the co-flowing air Reynolds number causes a reduction in the flame length. At Re$_c$ greater than about 1500, the flame mode becomes transitional and the effect of co-flowing air Reynolds number on the flame length is reversed—larger Re$_a$ induces larger flame length for a fixed Re$_c$. The increasing rate of the flame length with the increase of Re$_c$ in the transitional flame regime becomes significantly lower than that in the attached flame regime. As the flame is lifted, the flame length does not increase significantly with the increase of Re$_c$ and would approach to a value of about 57w as Re$_c$ is greater than about 3000 at Re$_a$ = 1489 and about 48w at Re$_a$ = 484.

For comparison, the length of the plane jet flame (without

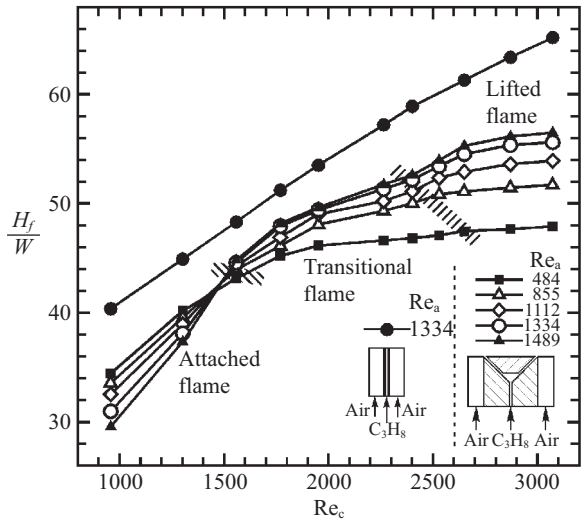

Fig. 6. Non-dimensional flame length at various Re_a.

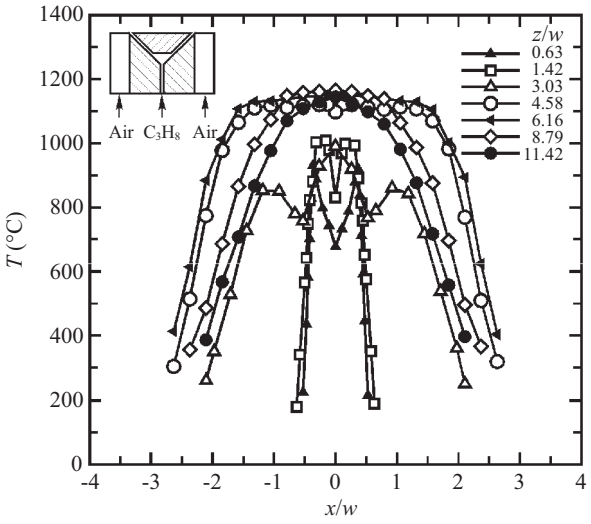

Fig. 7. Lateral temperature distributions of attached flame at various attitudes. Re_c = 957 and Re_a = 1334.

bifurcation) at Re_a = 1334 is noted in Fig. 6. The length of the bifurcated flame at Re_a = 1334 is apparently shorter than that of the plane jet flame. At differences are about 30%, 11%, and 17% at Re_a = 957, 2263, and 3072. The mixing and entrainment effects of the bifurcated flame are drastically increased by alteration of flow structure, and therefore the flame length is significantly reduced.

4. Temperature Distributions

Fig. 7 shows the temperature distributions of an attached flame at various levels at Re_c = 957 and Re_a = 1334. At the lower levels (z/w < 4.58), central dips appear in the temperature profiles since the flame has not combined yet. At the level $z/w \approx 3.03$, the temperature distribution becomes wide. This corresponds to the sudden widening of flame shown in Fig. 2(a). At the levels higher than z/w > 4.58, the central dips disappear, which indicates that the primary reaction almost finishes. The central region presents wide plateaus of high temperatures. The maximum temperature the flame attains is about 1150°C.

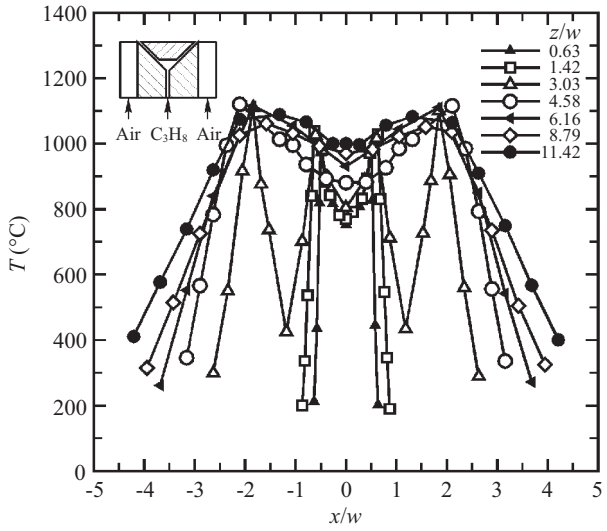

Fig. 8. Lateral temperature distributions of transitional flame at various attitudes. Re_c = 2401 and Re_a = 1334.

Fig. 8 shows temperature distributions of a transitional flame at various levels at Re_c = 2401 and Re_a = 1334. For all levels z/w < 11.42, the central region presents apparently lower temperatures than the peak values standing at two sides, which shows the feature of diffusion flame. The low temperature appearing at the center increases with the increase of z/w. The flame has not combined yet at the levels z/w < 11.42. The flame distributions are wider than those of the attached flame shown in Fig. 7. The temperature distributions at the levels $z/w \geq 3.03$ are specifically wider than those at $z/w \leq 1.42$. This corresponds to the sudden widening of flame shown in Fig. 2(b) at $z/w \approx 2$. The maximum temperature the flame attains is about 1100°C.

Fig. 9 shows the temperature distributions of a lifted flame at various levels of the flame at Re_c = 3072 and Re_a = 1334. At the lower levels, z/w < 4.58, central dips appear in the temperature profiles since the flame has not combined yet. At the level $z/w \approx 1.42$, the temperature distribution becomes wide. This level is lower than the critical level of the attached and transitional flames because the mergence point of the lifted flame appears at the lower level. At the levels higher than z/w > 8.79, the central region presents wide plateaus of high temperatures, which indicates that the primary reaction almost finishes at the level $z/w \approx 8.79$. The spread widths of the temperature profiles for the lifted flame are apparently larger than those of the attached and transition flames (Figs. 7 and 8), and therefore indicate that the flame width of the lifted flame is wider than that of the attached and transitional flames. The maximum temperature the flame attains is about 1050°C.

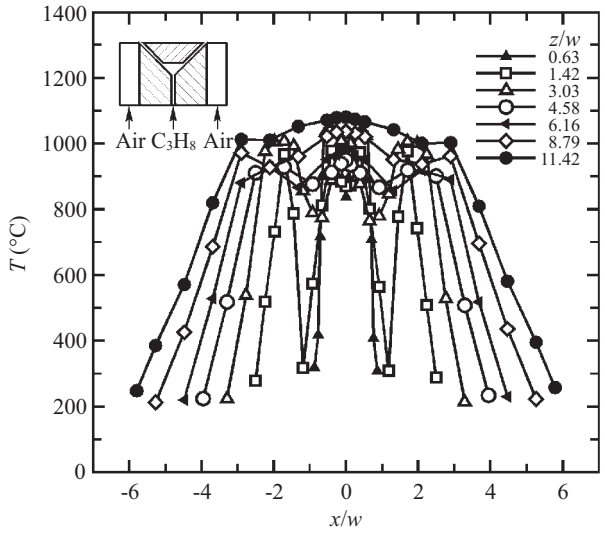

Fig. 9. Lateral temperature distributions of lifted flame at various attitudes. Re_c = 3072 and Re_a = 1334.

From Figs. 7-9, the widths of the temperature distributions increase with the increase of Re_c. However the maximum temperatures decrease with the increase of Re_c.

IV. CONCLUSIONS

By attaching a specially designed V-shaped bluff-body burner to a plane jet, the flame appearances and temperature distributions were drastically changed. The flame appearance, flame lengths, and temperature distributions of the bifurcated jets were examined experimentally. The following conclusions were made from the results of this study.

(1) Three characteristic flame modes—attached flame, transitional flame, and lifted flame—in the domain of Re_c and Re_a are identified.

(2) The flame length and width increase with increasing Re_c at a fixed Re_a. The length of the bifurcated flame is significantly shorter than that of the plane jet flame. The reduction is induced by the enhancement in the mixing and entrainment effects of the bifurcated flame, which are induced by alteration of flow structure.

(3) In the attached flame regime, increasing the co-flowing air Reynolds number causes a reduction in the flame length. While in the transitional and lifted flame regimes, increasing the co-flowing air Reynolds number decreases the flame length.

REFERENCES

1. Fiedler, H. E. and Mensing, P., "The plane turbulent shear layer with periodic excitation," *Journal of Fluid Mechanics*, Vol. 150, pp. 281-309 (1985).
2. Friedman, J., Bennet, W. J., and Zwick, E. B., "The engineering application of combustion research to ramjet engines," *Fourth Symposium (International) on Combustion*, Vol. 4, No. 1, pp. 756-764 (1953).
3. Fujisawa, N., Nakamura, K., and Srinivas, K., "Interaction of two parallel plane jets of different velocities," *Journal of Visualization*, Vol. 7, No. 2, pp. 135-142 (2004).
4. Laufer, J. and Yen, T. C., "Noise generation by a low Mach number jet," *Journal of Fluid Mechanics*, Vol. 134, pp. 1-31 (1983).
5. Lefebvre, A. H., *Gas Turbine Combustion*, Hemisphere, New York (1983).
6. Longwell, J. P., "Combustion problems in ramjets," *Fifth Symposium (International) on Combustion*, Vol. 5, No. 1, pp. 48-56 (1955).
7. Longwell, J. P., Chenevey, J. E., Clark, W. W., and Frost, E. E., "Flame stabilization by baffles in a high velocity gas stream," *Third Symposium on Combustion and Flame and Explosion Phenomena*, Vol. 3, No. 1, pp. 40-44 (1949).
8. Marsters, G. F., "Interaction of two plane, parallel jets," *AIAA Journal*, Vol. 15, No. 12, pp. 1756-1762 (1977).
9. Miller, D. R. and Comings, E. W., "Force-moment fields in a dual-jet flow," *Journal of Fluid Mechanics*, Vol. 7, pp. 237-256 (1960).
10. Nasr, A. and Lai, J. C. S., "Comparison of flow characteristics in the near field of two parallel plane jets and an offset plane jet," *Physics of Fluids*, Vol. 9, No. 10, pp. 2919-2931 (1997).
11. Nicholson, H. M. and Field, J. P., "Some experimental techniques for the investigation of the mechanism of flame stabilization in the wakes of bluff bodies," *Third Symposium on Combustion and Flame and Explosion Phenomena*, Vol. 3, No. 1, pp. 44-68 (1949).
12. Schadow, K. C. and Gutmark, E., "Combustion instability related to vortex shedding in dump combustors and their passive control," *Progress in Energy and Combustion Science*, Vol. 18, pp. 117-132 (1992).
13. Wright, F. H. and Zukoski, E. E., "Flame spreading from bluff-body flameholders," *Eighth Symposium (International) on Combustion*, Vol. 8, No. 1, pp. 933-943 (1961).